

# S2R-ViT for Multi-Agent Cooperative Perception: Bridging the Gap from Simulation to Reality

Jinlong Li<sup>1</sup>, Runsheng Xu<sup>2</sup>, Xinyu Liu<sup>1</sup>, Baolu Li<sup>1</sup>, Qin Zou<sup>3</sup>, Jiaqi Ma<sup>2</sup>, Hongkai Yu<sup>1\*</sup>

**Abstract**—Due to the lack of real multi-agent data and time-consuming of labeling, existing multi-agent cooperative perception algorithms usually select the simulated sensor data for training and validating. However, the perception performance is degraded when these simulation-trained models are deployed to the real world, due to the significant domain gap between the simulated and real data. In this paper, we propose the *first* Simulation-to-Reality transfer learning framework for multi-agent cooperative perception using a novel Vision Transformer, named as S2R-ViT, which considers both the Implementation Gap and Feature Gap between simulated and real data. We investigate the effects of these two types of domain gaps and propose a novel uncertainty-aware vision transformer to effectively relieve the Implementation Gap and an agent-based feature adaptation module with inter-agent and ego-agent discriminators to reduce the Feature Gap. Our intensive experiments on the public multi-agent cooperative perception datasets OPV2V and V2V4Real demonstrate that the proposed S2R-ViT can effectively bridge the gap from simulation to reality and outperform other methods significantly for point cloud-based 3D object detection.

## I. INTRODUCTION

The recent advancement in cooperative perception systems show potentiality to overcome the limitation of single agent perception, which would suffer from many real-world challenges, *e.g.*, perceiving range and occlusion [1]. Cooperative perception system can significantly improve the perception performance in the complex traffic environment by leveraging the Vehicle-to-Vehicle (V2V) communication technology to share the visual information [2], [3]. Recently, multi-agent perception systems have shown great potential in overcoming the limitations of single-agent perception, which often face challenges such as limited perceiving range and occlusion [1]. By leveraging Vehicle-to-Vehicle (V2V) communication technology to share visual information, multi-agent perception systems can significantly enhance perception performance in complex traffic environments [2], [3]. Current multi-agent perception methods employ three approaches for information sharing in V2V communication: sharing raw sensing data, sharing intermediate features, and sharing detected outputs.

However, due to the labor-intensive nature of point cloud data labeling, most models achieve excellent performance by training and testing on large-scale simulated datasets such as OPV2V [3]. These models assume homogeneous feature distributions between training and testing data. Nevertheless,

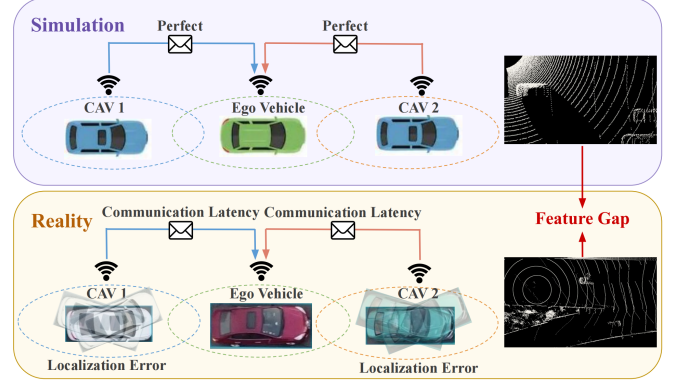


Fig. 1: Illustration of the domain gap (*Implementation Gap*, *Feature Gap*) for multi-agent cooperative perception from simulation to reality. Here we use V2V cooperative perception in autonomous driving as an example.

this assumption may fail when deploying the model in real-world scenarios. As depicted in Fig. 1, state-of-the-art methods trained on simulated OPV2V data exhibit good detection performance in simulation but suffer from a significant drop in performance when tested on real data due to the domain shift between simulation and reality.

Furthermore, data labeling for cooperative perception systems is particularly time-consuming and expensive. Compared to single-agent perception systems, multi-agent perception systems incur significantly higher costs, as labelers need to annotate multiple sensor views, making scalability difficult. In this paper, our research focuses on utilizing labeled simulated data and unlabeled real-world data to reduce domain discrepancies in cooperative 3D detection. However, it is widely acknowledged that a significant domain gap exists between simulated and real-world data distributions. We observe this domain discrepancy in V2V multi-agent perception from two perspectives:

- **Implementation Gap:** As shown in Fig. 1, different with the ideal simulation setting, the multiple agents might have localization (positional and heading) errors due to the unavoidable GPS errors and communication latency (time delay) during the real-world agent-to-agent communication.
- **Feature Gap:** As illustrated in Fig. 1, the point cloud feature distribution in real world might differ significantly with that of the simulated data, such as more complex driving scenarios, different LiDAR channel numbers, mixed traffic flow, various point cloud vari-

<sup>1</sup>Cleveland State University, Cleveland Vision & AI Lab. <sup>2</sup>University of California, Los Angeles, UCLA Mobility Lab. <sup>3</sup>Wuhan University.

\*Corresponding Author: h.yu19@csuohio.edu

ations, and so on.

In this paper, we choose the task of Vehicle-to-Vehicle (V2V) Cooperative Perception for the point cloud-based 3D object detection as algorithm development. To address these two dominant distinctions, we propose the first Simulation-to-Reality transfer learning framework using a novel Vision Transformer, named S2R-ViT. This framework effectively aligns the domain shift from simulation to reality, as illustrated in Figure 2. Specifically, the framework takes labeled point cloud data from the source domain and unlabeled data from the target domain as input. It comprises two key components: the Simulation-to-Reality Uncertainty-aware Vision Transformer (S2R-UViT) and the Simulation-to-Reality Agent-based Feature Adaptation (S2R-AFA). To mitigate the effect of the implementation gap, S2R-UViT employs two multi-head self-attention branches (LG-MSA), incorporating both local-based and global-based attention to enhance feature interactions across all agents' spatial positions. Additionally, a Uncertainty-Aware Module (UAM) is proposed to assign weights to the ego-agent feature, considering uncertain factors arising from the shared features of other agents. Moreover, to bridge the feature gap, we introduce a S2R-AFA that includes inter-agent and ego-agent discriminators, enabling S2R-ViT to generate robust, domain-invariant representations. We conducted extensive experiments on two public datasets, namely OPV2V and V2V4Real, and the results demonstrate the superior performance of our proposed method. Our contributions can be summarized as follows:

- To the best of our knowledge, we propose the **first research** on multi-agent cooperative perception from simulation to reality and study two types of domain gaps, *i.e.* Implementation Gap and Feature Gap, for point cloud-based 3D object detection in the real world.
- We propose a novel uncertainty-aware vision transformer to effectively relieve the uncertainty in the Implementation Gap.
- We design an agent-based feature adaptation module that includes inter-agent and ego-agent discriminators to effectively reduce the Feature Gap between simulation and reality.
- We evaluate our proposed method on the large-scale simulated OPV2V dataset and the real V2V4Real dataset, whose experiments demonstrate our superior performance in point cloud-based 3D object detection.

## II. RELATED WORK

**Multi-Agent Cooperative Perception.** Current single-agent perception systems still suffer severely from refraction, occlusion, and long-range distance when they are deployed in the real world scenario [3], [4]. Multi-agent perception system can overcome these real-world challenge via Vehicle-to-Vehicle (V2V) communication technology to achieve the large-range perception performance, which has attracted the attention of many researchers. Instead of sharing raw sensing data or detected outputs, state-of-the-art methods usually

share the intermediate neural features computed from the sensor data, as they can achieve the best trade-off between accuracy and bandwidth requirements [1], [5]–[7]. V2VNet [2] employed a graph neural network to aggregate features extracted by LiDAR from each vehicle. When2com [7] utilizes a spatial confidence-aware communication strategy to use less communication to improve performance. OPV2V [3] utilized a self-attention module to fuse the received intermediate features. SyncNet [8] introduces a latency compensation module for time-domain synchronization. V2X-ViT [5] proposed a vision Transformer architecture to fuse features from vehicles and infrastructures. CoBEVT [9] proposed a fused axial attention mechanism that allows for local and global interactions across all views and agents to improve the performance. Although these methods have demonstrated impressive performance, all of them are implemented in the simulated data without considering the realistic domain gap issue in the real world. In this paper, we aim to fill this gap from simulation to realistic.

**Challenge in Multi-Agent.** Multi-Agent perception system has distinct advantages, but it also introduces some new challenges, *e.g.*, localization error, communication latency, lossy communication, adversarial attacks. These challenges can easily diminish the benefits of collaborations [5], [6], [10]. To ensure robustness and safety for Multi-Agent perception, V2X-ViT [5] first proposed to use a vision transformer for multi-agent perception and achieves robust performance under GPS error and communication delay. [11] proposes a pose regression module and consistency module before feature aggregation to correct pose errors. [7] proposes the first latency-aware collaborative perception system, which realizes a feature level synchronization. [12] investigates adversarial attacks in collaborative perception design a novel transfer attack approach in the intermediate collaborative perception. [10] proposes LC-aware Repair Network ensure the robustness of collaborative perception under lossy communication to recover features from other agents. To further develop Multi-Agent perception system, some available large-scale collaborative perception datasets are published, *e.g.*, simulated OPV2V dataset [3], which is collected with the co-simulating framework OpenCDA [4], and real-world V2V4Real dataset, which is collected by two vehicles equipped with multi-modal sensors driving together through diverse scenarios. However, Annotating multiple sensor views in real-world multi-agent perception is labor-consuming, which is main blockneck of multi-agent perception deployment. In this paper, We focus on cooperative 3D detection improvement in the real world by utilizing labelled simulated data and unlabelled real-world data, and we select the simulated OPV2V and real V2V4Real datasets for our experiments.

**Domain Adaptation for Point Cloud.** Time/Labor consuming for data annotation is the critical issue for deep learning method deployment in the real world, and data from different domains usually exists the large domain gap. Domain adaptation is utilized to solve these problems by adapting the model trained on a labeled source domain to address an

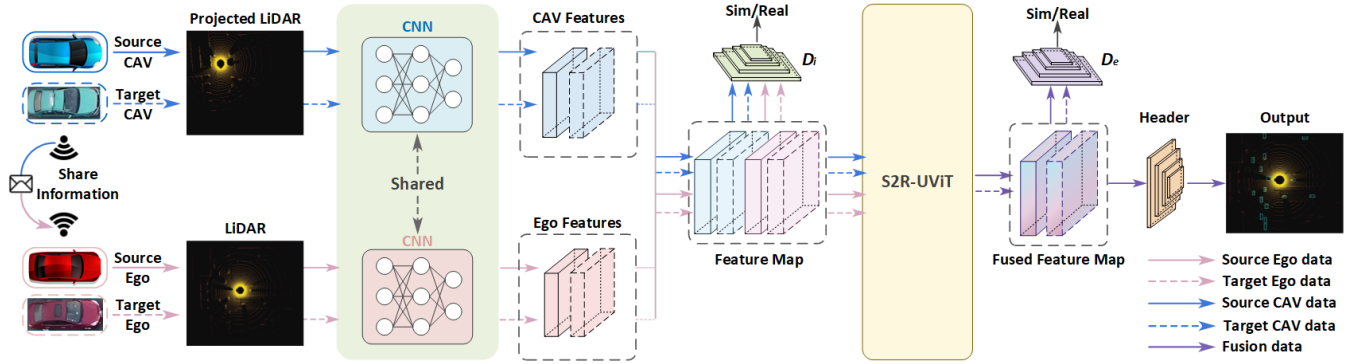


Fig. 2: Overview of proposed S2R-ViT multi-agent cooperative perception, which leverages S2R-UViT module to handle uncertainty in Implementation Gap and tackles the Feature Gap through S2R-AFA module including the inter-agent discriminator  $D_i$  and the ego-agent discriminator  $D_e$ . Source Domain: labeled simulated data, Target Domain: unlabeled real-world data.

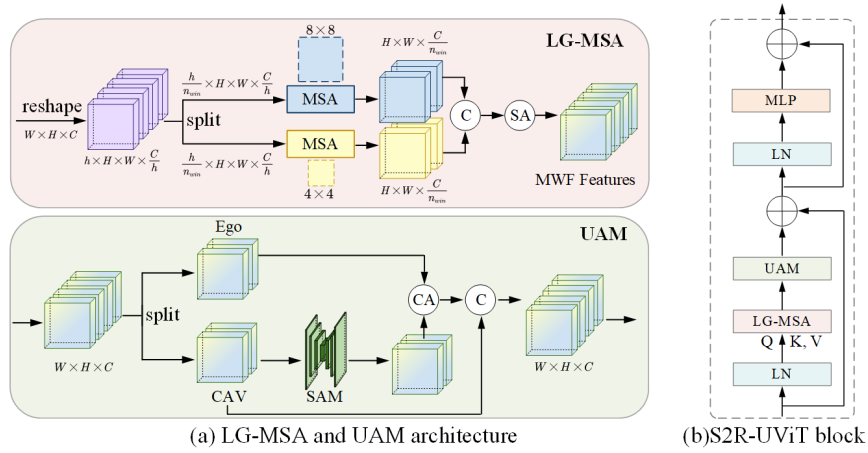


Fig. 3: Architecture of the proposed S2R-UViT: Simulation-to-Reality Uncertainty-aware Vision Transformer.

unlabeled target domain. Previous domain adaptation works mainly focus on the RGB camera-based data track [13]–[16], while more and more research have been proposed to solve domain adaptation in LiDAR-based data track [6], [17]–[19]. Specifically, A Sparse Voxel Completion Network [17] is designed to complete the 3D surfaces of a sparse point cloud, and uses local adversarial learning to model the surface prior. Semantic Point Generation (SPG) [18] is presented to enhance the reliability of LiDAR detectors against domain shifts to generates semantic points at the predicted foreground regions. CoSMix [19] is proposed for 3D LiDAR segmentation to mitigate the domain shift by creating two new intermediate domains of composite point clouds obtained by applying a novel mixing strategy at input level. [6] proposes a new Multi-agent Perception Domain Adaption (MPDA) framework, which is the first work to bridge the domain gap for multi-agent perception. In this paper, the agent-based domain Adaptation modules are proposed to align the domain gap for simulation to real on multi-agent perception system.

### III. METHODOLOGY

In this paper, we explore the domain adaptation for LiDAR-based 3D object detection from simulation to real. Our goal is to utilize a large number of existing simulated data with annotation and real data without any labels to reduce the domain discrepancy, improving the multi-agent perception capabilities of the connected automated vehicle in the real-world. The end-to-end unified pipeline, illustrated in Fig. 2, includes 1) V2V metadata sharing, 2) Feature extraction and sharing, 3) S2R-ViT, and 4) Detection head.

#### A. Overview of architecture

**1) V2V metadata sharing.** We select one of the CAVs as the ego vehicle to construct a spatial graph around it where each node is a CAV within the communication range. Upon receiving the relative pose and extrinsic of the ego vehicle, all the other CAVs nearby will project their own LiDAR information to the ego vehicle’s coordinate frame before feature extraction. **2) Feature extraction and sharing.** We leverage the anchor-based PointPillar method [20] to extract visual features from point clouds because of its low inference latency and optimized memory usage. the backbone extracts

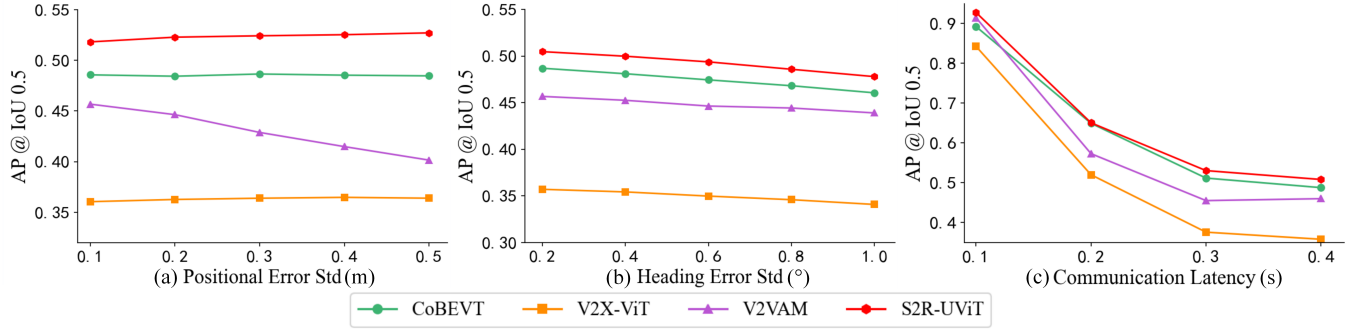


Fig. 4: Robustness to **Implementation-Gap scenario** including positional error, heading error, and communication latency on the CARLA Towns testing set of OPV2V [3] with *Noisy Setting*.

informative visual feature maps. Each CAV has its own LIDAR feature extraction module. The ego vehicle will receive the neighboring CAV feature maps after each CAV feature extraction. **3) S2R-ViT.** The intermediate features aggregated from other surrounding CAVs are fed into the major component of our framework. The proposed S2R-UViT and S2R-AFA modules will be revealed with details in Sec. III-B and Sec. III-C, respectively. **4) Detection head.** After receiving the final fused feature maps, two prediction headers are utilized for box regression and classification.

#### B. S2R-UViT: Simulation-to-Reality Uncertainty-aware Vision Transformer

Fusing the shared features from other multiple agents and eliminate the effect of implementation gaps requires both local and global interactions across all agents' spatial positions. Specifically, the other feature from neighboring CAVs often have different pose's size and head direction on the same object, local-based attention can care more about local details of feature information to do pixel-wise construction on these objects. Equally, the different CAVs also have different shift levels on the same scene, global-based attention can also help correct and repair the shift of the sharing traffic scenes. Inspired by Divide and Conquer Algorithm, the whole features are spilt into two branches (*i.e.*, local branch and global branch) to process by local-based and global-based attentions, respectively, then these two features are concatenated together and fed into a self-attention (SA) module to further capture local and global information. To enhance the feature from ego agent based on the shared other agent's information, a specific per-tensor mask, which is generated by an encoder-decoder architecture network, are optimized to reserve the value with high confident score in the mask by a Uncertainty-Aware Module (UAM), then mask multiplies with the ego feature to obtain the enhanced feature of ego-agent with considering all high confident spatial information of other agents.

Fig. 3 presents the architecture of S2R-UViT. Inspired by [21], [22], after retrieving the whole features  $F_{e,s} \in \mathbb{R}^{W \times H \times C}$  with spatial dimension  $W \times H$  from all agents ( $e$  is denoted ego-agent,  $s$  is denoted other-agent), we reshape it into  $F_{e,s}^l \in \mathbb{R}^{h \times H \times W \times \frac{C}{h}}$ . After that, we take  $h = 2$

and  $n_{win} = 2$ , the multi-head  $h$  of standard multi-head self attention module (MSA) [23] is evenly divided into 2 groups with two different window sizes, *i.e.*,  $Win_{size} = 4 \times 4$  is for the local branch and  $Win_{size} = 8 \times 8$  is for global branch. In *local branch*, the spilt feature  $F_{e,s}^l \in \mathbb{R}^{h \times H \times W \times \frac{C}{h}}$  is fed into the MSA with  $Win_{size} = 4 \times 4$  to enhance the local details of feature. In *global branch*, another spilt feature  $F_{e,s}^g \in \mathbb{R}^{h \times H \times W \times \frac{C}{h}}$  is fed into the MSA with  $Win_{size} = 8 \times 8$  to capture global feature information. Then we concat these two branch output features and do information fusion enhancement by a self attention module, to obtain the enhanced feature  $F_{e,s}^m \in \mathbb{R}^{W \times H \times C}$ , our LG-MSA is defined as follows,

$$F_{e,s}^1 = \text{Concat}(\text{MSA}_L(F_{e,s}^l), \text{MSA}_G(F_{e,s}^g)), \quad (1)$$

$$F_{e,s}^m = \text{SA}(F_{e,s}^1). \quad (2)$$

When receiving the enhanced feature  $F_{e,s}^m$  for all agents, we split them into ego agent feature  $F_e^m \in \mathbb{R}^{W \times H \times C}$  and other agent shared feature  $F_s^m \in \mathbb{R}^{W \times H \times C}$ . The shared feature  $F_s^m$  is as input into our spatial aware network (SAN), which can generate a spatial aware matrix  $M \in \mathbb{R}^{W \times H \times C}$  with the same size of input feature. Then spatial aware matrix  $M$  is generated and as the input for our Uncertainty-Aware Module (UAM), Which can keep values with high confidence and discard values with low confidence, and the spatial aware matrix  $M1$  with retaining high confidence is applied to  $F_e^m \in \mathbb{R}^{W \times H \times C}$  to produce the enhanced ego feature. Here we use the median as our threshold in UAM. Finally, the enhanced ego feature and other agent shared feature are concat together to obtain the output feature  $F_{e,s}^h \in \mathbb{R}^{W \times H \times C}$ , which could be simply formulated as

$$F_e^+ = \text{UAM}(\text{SAN}(F_s^m)) + F_e^m, \quad (3)$$

$$F_{e,s}^h = \text{Concat}(F_e^+, F_s^m), \quad (4)$$

Combining these local and global attention branches with typical designs of Transformers [21], [22], including Layer Normalization (LN), MLPs, and skip-connections, forms our proposed S2R Uncertainty-aware attention block, as shown in Fig. 3. The S2R-UViT block can be simply expressed as:

$$F_{e,s}^h = \text{S2RAttn}(\text{LN}(F_{e,s})) + F_{e,s}, \quad (5)$$



$$\hat{F}_{e,s}^h = \text{MLP}(\text{LN}(F_{e,s}^h)) + F_{e,s}^h, \quad (6)$$

where  $F_{e,s}^h$  and  $\hat{F}_{e,s}^h$  denote the output features of the S2RAttn module (*i.e.*, LG-MSA and UAM) and MLP module.

### C. S2R-AFA: Simulation-to-Reality Agent-based Feature Adaptation

Realistic collaboration scenarios often present complexities that differ from idealized situations. Specifically, the simulated OPV2V dataset utilizes a LiDAR sensor with 64 beams, resulting in mostly dense point clouds. On the other hand, the real V2V4Real dataset is collected using a Velodyne VLP-32 beam LiDAR sensor, leading to sparse point clouds. To align these domain gaps from simulated feature  $F_S$  and real feature  $F_T$ , we design two domain discriminators before and after fusion as shown in Fig. 2, where all agents feature  $F_S$  and  $F_T$  from the encoder are fed into the inter-agent discriminator  $D_i$  to classify whether which one is real or fake, and the fused ego features  $F'_S$  and  $F'_T$  from S2R-UViT also are classified into real or fake by the ego-agent discriminator  $D_e$ . Therefore, these two discriminators are optimized by the Agent-based Feature Adaptation loss  $\mathcal{L}_{AFA}$ :

$$\max_M \min_{D_{\{i,e\}}} \mathcal{L}_{AFA} = \mathbb{E}[D_{\{i,e\}}(F_T, F'_T)] + \mathbb{E}[1 - D_{\{i,e\}}(F_S, F'_S)], \quad (7)$$

where  $M$  is our whole model including encoder, S2R-UViT and detection header. After domain adaptation, our model  $M$  has the capability of extracting domain-invariant features.

For 3D object detection, we use the smooth L1 loss for bounding box regression and focal loss [24] for classification. The final loss is the combination of detection and Agent-based Feature Adaptation loss  $\mathcal{L}_{AFA}$  as follows,

$$\mathcal{L}_{total} = \mu \mathcal{L}_{det} + \lambda \mathcal{L}_{AFA}, \quad (8)$$

where  $\mu$  and  $\lambda$  are the balance coefficients within range  $[0, 1]$ .

## IV. EXPERIMENT

### A. Dataset

We conduct experiments on the two public benchmark datasets for V2V cooperative perception tasks including OPV2V [3] and V2V4Real [25]. **OPV2V** is a large-scale simulated dataset for V2V cooperative perception task, which is collected by CARLA and OpenCDA [4]. It contains 73 divergent scenes with various numbers of connected vehicles, and its training/validation/testing set is split into 6,764, 1,981, and 2,719 frames, respectively. **V2V4Real** is a real-world, large-scale, multi-modal dataset with diverse driving scenarios, which is collected by two vehicles drive simultaneously in Columbus, Ohio, USA. It's split into the train/validation/test set with 14,210/2,000/3,986 frames, respectively.

TABLE I: 3D detection performance on two OPV2V testing sets under **Implementation-Gap Scenario**. We show Average Precision (AP) at IoU=0.5, 0.7 on *Perfect Setting* and *Noisy Setting*, respectively. All methods are trained on *Perfect Setting*.

Models	Setting	V2V CARLA AP@0.5	Towns AP@0.7	V2V Culver City AP@0.5	City AP@0.7
No Fusion	Perfect	0.679	0.602	0.557	0.471
	Noisy	0.679	0.602	0.557	0.471
AttFuse [3]	Perfect	0.921	0.804	0.887	0.716
	Noisy	0.851	0.472	0.865	0.565
V2Vnet [2]	Perfect	0.915	0.828	0.884	0.757
	Noisy	0.845	0.413	0.868	0.617
F-cooper [1]	Perfect	0.907	0.81	0.893	0.746
	Noisy	0.842	0.479	0.881	0.624
V2X-ViT [5]	Perfect	0.902	0.792	0.903	0.764
	Noisy	0.801	0.395	0.882	0.606
CoBEVT [9]	Perfect	0.925	0.852	0.904	0.776
	Noisy	0.862	0.519	0.889	0.665
V2VAM [10]	Perfect	0.916	0.849	0.903	<b>0.794</b>
	Noisy	0.876	0.507	0.883	0.663
S2R-UViT	Perfect	<b>0.928</b>	<b>0.867</b>	<b>0.912</b>	0.768
	Noisy	<b>0.879</b>	<b>0.579</b>	<b>0.900</b>	<b>0.681</b>

### B. Experiments Setup

**Evaluation metrics.** The final 3D vehicle detection accuracy are selected as our performance evaluation. Following [3], [5], we set the evaluation range as  $x \in [-140, 140]$  meters,  $y \in [-40, 40]$  meters, where all CAVs are included in this spatial range, whose number is in the range of  $[1, 5]$  in the experiment. and we measure the accuracy with Average Precisions (AP) at Intersection-over-Union (IoU) threshold of 0.5 and 0.7.

**Experiment details.** In this work, we want to address the implementation gap and domain gap on LiDAR-based object detection and assess our model under two distinct settings:

- 1) **Implementation-Gap Scenario:** During the training, all models are trained in the perfect simulated OPV2V training set, then all of them are evaluated on OPV2V CARLA Towns and Culver City testing sets under two different setting (*e.g.*, *Perfect* and *Noisy*), respectively. We implement the *Noisy Setting* by following [5], the positional and heading noises of the transmitter are drawn from a Gaussian distribution with a default standard deviation of 0.2 m and  $0.2^\circ$  respectively, and communication latency is set to 100 ms for all the evaluated models. This Implementation-Gap Scenario only includes the Implementation Gap.
- 2) **Sim2Real Scenario:** We set the labeled training set of simulation dataset OPV2V [3] as the source domain and the unlabeled training set of the real-world dataset V2V4Real [25] as the target domain for all models during the training, by following the same setting in [25]. Then, all trained models are evaluated on the testing set of V2V4Real to report the performance. This Sim2Real

Scenario includes both the Implementation Gap and Feature Gap from simulation to reality.

Specifically, all models use the PointPillar [26] as the backbone with the voxel resolution of 0.4 m for both height and width. We adopt Adam optimizer [27] with an initial learning rate of  $10^{-3}$  and steadily decay it every 10 epochs using a factor of 0.1. We follow the same hyperparameters in V2X-ViT [5], and all models are trained on two RTX 3090 GPUs.

**Compared methods.** We evaluate six state-of-the-art V2V methods in this paper, which use *Intermediate Fusion* as the main fusion strategy: CoBEVT [9], F-Cooper [1], V2VNet [2], OPV2V [3], V2VAM [10] and V2X-ViT [5] (see Sec.II for detailed descriptions). To demonstrate the significant effect of implementation gap and domain gap, we first train these methods on perfect setting of OPV2V training set. Then, these methods are evaluated on *Noisy Setting* of OPV2V testing set and V2V4Real testing set to assess their performance. In addition, to show the effectiveness of our proposed domain adaptation modules on *Feature-Gap scenario*, two domain adaptation methods *i.e.*, gradient reverse layer (GRL) [28] and adversarial gradient reverse layer (AdvGRL) [14] are utilized to backpropagate the gradient to assist the model for generating domain-invariant features by two domain classifiers including feature-level and object-level classifiers.

### C. Quantitative Evaluation

**Performance in Implementation-Gap Scenario.** Table I shows the performance comparison of current state-of-art methods on *Implementation-Gap Scenario*, where all methods are evaluated on *Perfect Setting* and *Noisy setting*, respectively. Under the *Perfect Setting*, all cooperative perception methods achieve better performance than the baseline *NO Fusion* by a large margin. Nevertheless, when these methods deployed on the *Noisy Setting* scenario, which have the implementation gap with the *Perfect Setting* scenario, the V2X-ViT [5], CoBEVT [9], and V2VAM [10] drop 39.7%, 33.3%, and 34.2% on for AP@0.7 on V2V CARLA Towns testing set. Clearly, Due to all methods unseen these data with V2V implementation gap in the training phase, their detection performance is even worse than single-agent perception baseline *NO Fusion* on for AP@0.7 on V2V CARLA Towns testing set, which indicates the highly negative impacts by V2V implementation gap. While our proposed S2R-UViT achieves the mostly best performance under both *Perfect Setting* and *Noisy Setting* scenario, which is highlighted in Table I. To assess the models' sensitivity on different *Implementation-Gap Scenario*, we conduct the experiments on the V2V CARLA Towns testing set of OPV2V dataset with the difference of *Noisy Setting*. The result of Fig. 4 depicts the robustness of S2R-UViT against implementation gap, when the performance of other fusion methods significantly degrades. The result of Table I indicates that our proposed S2R-UViT with LG-MSA and Uncertainty-Aware Module can eliminate the effect of implementation gap by reserving high confident score tensors.

TABLE II: 3D detection performance on V2V4Real testing set under *Sim2Real Scenario*. All methods with domain adaptation are trained following setting in *Sim2Real Scenario*. S2R-UViT w/ S2R-AFA indicates our S2R-ViT.

Method	V2VReal test	
	AP@IoU=0.5	AP@IoU=0.7
No Fusion (Supervised)	0.398	0.220
AttFuse [3]	0.225	0.094
AttFuse w/ GRL	0.356	0.139
AttFuse w/ AdvGRL	0.366	0.137
V2VNet [2]	0.268	0.108
V2VNet w/ GRL	0.376	0.122
V2VNet w/ AdvGRL	0.358	0.103
F-Cooper [1]	0.236	0.091
F-Cooper w/ GRL	0.372	0.116
F-Cooper w/ AdvGRL	0.364	0.135
V2X-ViT [5]	0.274	0.103
V2X-ViT w/ GRL	0.395	0.156
V2X-ViT w/ AdvGRL	0.401	0.161
CoBEVT [9]	0.334	0.130
CoBEVT w/ GRL	0.398	0.163
CoBEVT w/ AdvGRL	0.393	0.163
V2VAM [10]	0.332	0.120
V2VAM w/ GRL	0.390	0.146
V2VAM w/ AdvGRL	0.401	0.161
S2R-UViT	<b>0.367</b>	<b>0.138</b>
S2R-UViT w/ GRL	0.414	0.141
S2R-UViT w/ AdvGRL	0.414	0.157
S2R-UViT w/ S2R-AFA	<b>0.441</b>	<b>0.170</b>

**Performance in Sim2Real Scenario.** The result of 3D object detection on V2V4Real testing set on *Sim2Real Scenario* is presented in Table II. Among all intermediate fusion methods without any domain adaptation methods, our proposed S2R-UViT achieves the best performance by eliminating the implementation gap of the real V2VReal testing set. After applying the domain adaptation methods *e.g.*, GRL [28] and AdvGRL [14], all methods have the improvement of performance. For example, V2X-ViT improved by 12.1%/5.3% for AP@0.5/0.7 with GRL, and 12.7%/5.8% for AP@0.5/0.7 with AdvGRL. Our proposed S2R-ViT with S2R-AFA achieves the 44.1%/17.0% for AP@0.5/0.7 as the best performance with improvement of 7.4%/3.2% than S2R-UViT without DA. The performance of S2R-UViT on AP@0.5 is better than *NO Fusion (Supervised)*, which is a supervised learning model trained on V2V4Real training set with labels. Further, we visualize some 3D object detection results on V2V4Real testing set under *Sim2Real Scenario*, as shown in Fig. 5. Obviously, Our proposed S2R-AFA can effectively attribute the capability of S2R-ViT to generate more generalization feature representations.

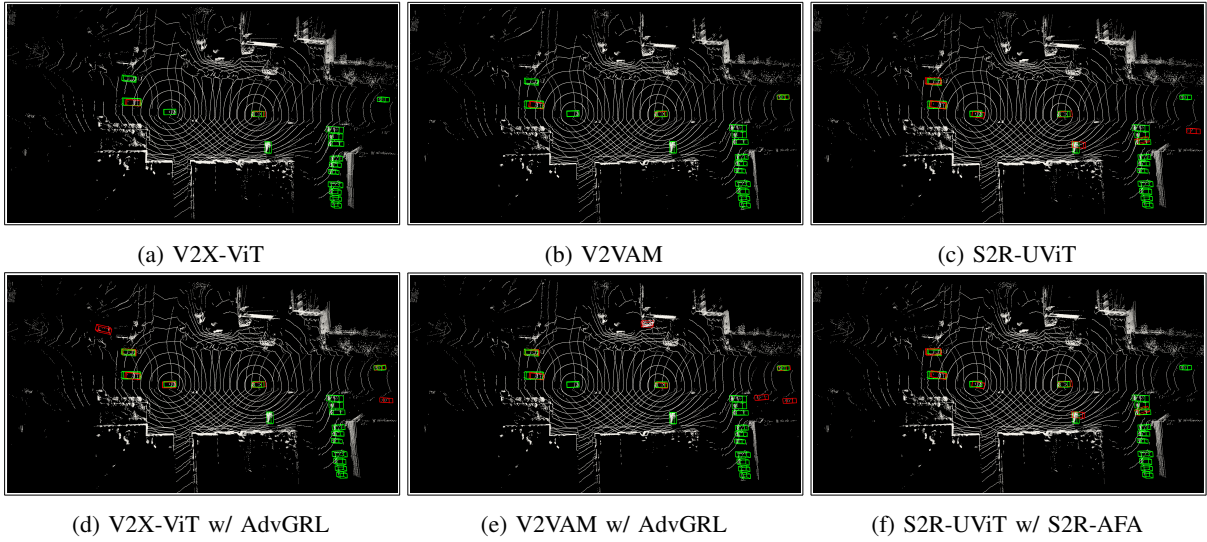


Fig. 5: Visualization of point cloud-based 3D object detection. Green and red 3D bounding boxes represent the ground truth and prediction respectively. S2R-UViT w/ S2R-AFA indicates our S2R-ViT, which yields more accurate detection results.

**Ablation Study.** As Table II depicts, all of our proposed components in S2R-ViT have contributed to more accurate detection performance. Specifically, our S2R-UViT achieves the best detection performance among all intermediate fusion methods, which is 3.3% and 0.8% higher than the second-best performance model CoBEVT in AP@0.5 and AP@0.7 respectively. Adding our S2R-AFA, our proposed S2R-ViT achieves 44.1% and 17.0% in AP@0.5 and AP@0.7, with the improvement of 6.4% in AP@0.5 and 3.2% in AP@0.7.

## V. CONCLUSIONS

This paper is the first work that investigates the domain gap on multi-agent cooperation perception from simulation to reality, specifically focusing on the implementation gap and feature gap in point cloud-based 3D object detection. Based on the analysis, we present the first Simulation-to-Reality transfer learning framework using a novel Vision Transformer, named S2R-ViT to mitigate these two types of domain gaps, which mainly contain an Uncertainty-aware Vision Transformer and an Agent-based Feature Adaptation module. The results demonstrate that our proposed method achieves the best performance on the V2V4Real dataset. This research presents a significant step forward in providing valuable insights into multi-agent cooperation perception from simulation to realistic.

## REFERENCES

- [1] Q. Chen, X. Ma, S. Tang, J. Guo, Q. Yang, and S. Fu, “F-cooper: Feature based cooperative perception for autonomous vehicle edge computing system using 3d point clouds,” in *ACM/IEEE Symposium on Edge Computing*, 2019, pp. 88–100.
- [2] T.-H. Wang, S. Manivasagam, M. Liang, B. Yang, W. Zeng, and R. Urtasun, “V2vnet: Vehicle-to-vehicle communication for joint perception and prediction,” in *European Conference on Computer Vision*. Springer, 2020, pp. 605–621.
- [3] R. Xu, H. Xiang, X. Xia, X. Han, J. Li, and J. Ma, “Opv2v: An open benchmark dataset and fusion pipeline for perception with vehicle-to-vehicle communication,” in *International Conference on Robotics and Automation*. IEEE, 2022, pp. 2583–2589.
- [4] R. Xu, H. Xiang, X. Han, X. Xia, Z. Meng, C.-J. Chen, C. Correa-Jullian, and J. Ma, “The openca open-source ecosystem for cooperative driving automation research,” *IEEE Transactions on Intelligent Vehicles*, pp. 1–13, 2023.
- [5] R. Xu, H. Xiang, Z. Tu, X. Xia, M.-H. Yang, and J. Ma, “V2x-vit: Vehicle-to-everything cooperative perception with vision transformer,” in *European Conference on Computer Vision*. Springer, 2022, pp. 107–124.
- [6] R. Xu, J. Li, X. Dong, H. Yu, and J. Ma, “Bridging the domain gap for multi-agent perception,” in *International Conference on Robotics and Automation*, 2023.
- [7] Y. Hu, S. Fang, Z. Lei, Y. Zhong, and S. Chen, “Where2comm: Communication-efficient collaborative perception via spatial confidence maps,” in *Advances in Neural Information Processing Systems*, 2022.
- [8] Z. Lei, S. Ren, Y. Hu, W. Zhang, and S. Chen, “Latency-aware collaborative perception,” in *European Conference on Computer Vision*. Springer, 2022, pp. 316–332.
- [9] R. Xu, Z. Tu, H. Xiang, W. Shao, B. Zhou, and J. Ma, “Cobevt: Cooperative bird’s eye view semantic segmentation with sparse transformers,” in *Conference on Robot Learning*, 2022.
- [10] J. Li, R. Xu, X. Liu, J. Ma, Z. Chi, J. Ma, and H. Yu, “Learning for vehicle-to-vehicle cooperative perception under lossy communication,” *IEEE Transactions on Intelligent Vehicles*, vol. 8, no. 4, pp. 2650–2660, 2023.
- [11] N. Vaideluvu, M. Ren, J. Tu, J. Wang, and R. Urtasun, “Learning to communicate and correct pose errors,” in *Conference on Robot Learning*. PMLR, 2021, pp. 1195–1210.
- [12] J. Tu, T. Wang, J. Wang, S. Manivasagam, M. Ren, and R. Urtasun, “Adversarial attacks on multi-agent communication,” in *IEEE International Conference on Computer Vision*, 2021, pp. 7768–7777.
- [13] J. Li, Z. Xu, L. Fu, X. Zhou, and H. Yu, “Domain adaptation from daytime to nighttime: A situation-sensitive vehicle detection and traffic flow parameter estimation framework,” *Transportation Research Part C: Emerging Technologies*, vol. 124, p. 102946, 2021.
- [14] J. Li, R. Xu, J. Ma, Q. Zou, J. Ma, and H. Yu, “Domain adaptive object detection for autonomous driving under foggy weather,” in *IEEE Winter Conference on Applications of Computer Vision*, 2023, pp. 612–622.
- [15] P. Oza, V. A. Sindagi, V. V. Sharmini, and V. M. Patel, “Unsupervised domain adaptation of object detectors: A survey,” *IEEE Transactions on Pattern Analysis and Machine Intelligence*, 2023.
- [16] L. Hoyer, D. Dai, H. Wang, and L. Van Gool, “Mic: Masked image consistency for context-enhanced domain adaptation,” in *Proceedings of the IEEE/CVF Conference on Computer Vision and Pattern Recognition*, 2023, pp. 11 721–11 732.
- [17] L. Yi, B. Gong, and T. Funkhouser, “Complete & label: A domain

- adaptation approach to semantic segmentation of lidar point clouds,” in *Proceedings of the IEEE/CVF conference on computer vision and pattern recognition*, 2021, pp. 15 363–15 373.
- [18] Q. Xu, Y. Zhou, W. Wang, C. R. Qi, and D. Anguelov, “Spg: Unsupervised domain adaptation for 3d object detection via semantic point generation,” in *Proceedings of the IEEE/CVF International Conference on Computer Vision*, 2021, pp. 15 446–15 456.
  - [19] C. Saltori, F. Galasso, G. Fiameni, N. Sebe, E. Ricci, and F. Poiesi, “Cosmix: Compositional semantic mix for domain adaptation in 3d lidar segmentation,” in *European Conference on Computer Vision*. Springer, 2022, pp. 586–602.
  - [20] A. H. Lang, S. Vora, H. Caesar, L. Zhou, and O. Beijbom, “Pointpillars: Fast encoders for object detection from point clouds,” in *IEEE Conference on Computer Vision and Pattern Recognition*, 2019.
  - [21] Z. Liu, Y. Lin, Y. Cao, H. Hu, Y. Wei, Z. Zhang, S. Lin, and B. Guo, “Swin transformer: Hierarchical vision transformer using shifted windows,” in *Proceedings of the IEEE/CVF international conference on computer vision*, 2021, pp. 10 012–10 022.
  - [22] P. Ren, C. Li, G. Wang, Y. Xiao, Q. Du, X. Liang, and X. Chang, “Beyond fixation: Dynamic window visual transformer,” in *Proceedings of the IEEE/CVF Conference on Computer Vision and Pattern Recognition*, 2022, pp. 11 987–11 997.
  - [23] A. Dosovitskiy, L. Beyer, A. Kolesnikov, D. Weissenborn, X. Zhai, T. Unterthiner, M. Dehghani, M. Minderer, G. Heigold, S. Gelly, J. Uszkoreit, and N. Houlsby, “An image is worth 16x16 words: Transformers for image recognition at scale,” in *International Conference on Learning Representations*, 2021. [Online]. Available: <https://openreview.net/forum?id=YicbFdNTTy>
  - [24] T.-Y. Lin, P. Goyal, R. Girshick, K. He, and P. Dollár, “Focal loss for dense object detection,” in *IEEE International Conference on Computer Vision*, 2017, pp. 2980–2988.
  - [25] R. Xu, X. Xia, J. Li, H. Li, S. Zhang, Z. Tu, Z. Meng, H. Xiang, X. Dong, R. Song, *et al.*, “V2v4real: A real-world large-scale dataset for vehicle-to-vehicle cooperative perception,” in *Proceedings of the IEEE/CVF Conference on Computer Vision and Pattern Recognition*, 2023, pp. 13 712–13 722.
  - [26] A. H. Lang, S. Vora, H. Caesar, L. Zhou, J. Yang, and O. Beijbom, “Pointpillars: Fast encoders for object detection from point clouds,” in *IEEE Conference on Computer Vision and Pattern Recognition*, 2019, pp. 12 697–12 705.
  - [27] I. Loshchilov and F. Hutter, “Decoupled weight decay regularization,” in *International Conference on Learning Representations.*, 2017.
  - [28] Y. Ganin and V. Lempitsky, “Unsupervised domain adaptation by backpropagation,” in *International Conference on Machine Learning*. PMLR, 2015, pp. 1180–1189.